

Alignment of photoions far from threshold

Romith Das, Chuanyong Wu, A. G. Mihill, E. D. Poliakoff, Kwanghsi Wang, and V. McKoy

Citation: *The Journal of Chemical Physics* **101**, 5402 (1994); doi: 10.1063/1.468408

View online: <http://dx.doi.org/10.1063/1.468408>

View Table of Contents: <http://scitation.aip.org/content/aip/journal/jcp/101/6?ver=pdfcov>

Published by the AIP Publishing

Articles you may be interested in

[Control of thermocapillary instabilities far from threshold](#)

Phys. Fluids **17**, 104109 (2005); 10.1063/1.2111144

[Bond energies of CaAr + , CaKr + , and CaXe + from resonant two-color photoionization thresholds](#)

J. Chem. Phys. **107**, 4451 (1997); 10.1063/1.474807

[Photoion rotational distributions from near-threshold to deep in the continuum](#)

J. Chem. Phys. **103**, 1773 (1995); 10.1063/1.469751

[New method to determine the photoionization threshold energy of a deep level from photocapacitance](#)

Appl. Phys. Lett. **25**, 572 (1974); 10.1063/1.1655315

[Sensitized Photoionization in Far Ultraviolet](#)

J. Chem. Phys. **26**, 715 (1957); 10.1063/1.1743387

The logo for AIP APL Photonics. It features the letters 'AIP' in a large, white, sans-serif font, followed by a vertical yellow bar and the words 'APL Photonics' in a smaller, white, sans-serif font. The background is a red gradient with a bright yellow sunburst effect in the center.

APL Photonics is pleased to announce
Benjamin Eggleton as its Editor-in-Chief



LETTERS TO THE EDITOR

The Letters to the Editor section is divided into four categories entitled Communications, Notes, Comments, and Errata. Communications are limited to three and one half journal pages, and Notes, Comments, and Errata are limited to one and three-fourths journal pages as described in the Announcement in the 1 July 1994 issue.

COMMUNICATIONS

Alignment of photoions far from threshold

Romith Das,^{a)} Chuanyong Wu,^{a)} A. G. Mihill,^{b)} and E. D. Poliakoff^{a),c)}
Louisiana State University, Baton Rouge, Louisiana 70803

Kwanghsi Wang and V. McKoy
Arthur Amos Noyes Laboratory of Chemical Physics,^{d)} California Institute of Technology,
Pasadena, California 91125

(Received 3 June 1994; accepted 12 July 1994)

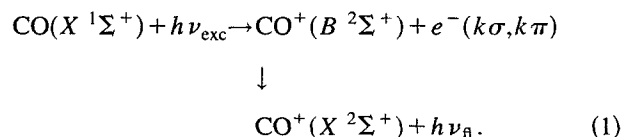
We present results of measurements and calculations of the alignment for $\text{CO}^+(B^2\Sigma^+)$ photoions over an extended energy range ($0 \leq E_k \leq 210$ eV). The polarization of $\text{CO}^+(B^2\Sigma^+ \rightarrow X^2\Sigma^+)$ fluorescence indicates that the photoions retain significant alignment even at high energies. Agreement between the measured and calculated polarization of the fluorescence is excellent.

When a molecule is photoionized, the photoelectron can exit in alternative continuum channels that reflect the symmetry of the molecule.¹ For example, an electron can be ejected from the 4σ orbital of CO into either a $k\sigma$ or a $k\pi$ orbital which represent degenerate pathways in the molecular electronic continuum. It has usually been assumed, either explicitly¹ or implicitly, that such a molecular photoionization process becomes atomlike at higher photon energies, and that the photoelectron will not show any preference for exiting along the molecular axis (the $k\sigma$ channel) as opposed to perpendicular to it (the $k\pi$ channel). However, to date it has not been possible to test this assumption because of experimental constraints. The relative strengths of these pathways cannot be determined from measurements of partial photoionization cross sections because the cross sections are the unresolved sums of all the dipole strengths. Similarly, these relative strengths cannot be extracted from photoelectron angular distributions due to interference among alternative partial waves making up the photoelectron angular distributions.²

The relative contributions of the degenerate pathways may be determined by measuring the *alignment* of the ion. If the ions are produced by fluorescing electronically excited states, then it is possible to determine the alignment, and consequently the relative strengths of alternative channels, by measuring the polarization of the fluorescence.³⁻⁸ While several investigations have exploited fluorescence polarization to disentangle the dynamics of complex photoionization events over limited spectral ranges, the present study is the first to do so over a large range of photon energies. The results provide a global view of the ionization dynamics that is illuminating, and in some respects, surprising. In particular, we find that the alignment of the photoions does not approach zero¹ as the photoelectron kinetic energy exceeds the ionization threshold by more than 200 eV. This implies that the molecular character of the ionization dynamics persists even at the highest measurable energies, in stark contrast to earlier expectations. The wide spectral coverage of

the current study provides a basis for investigating the validity of such pictures.

The experimental procedure has been described previously,¹ and is reviewed briefly here. The experimental geometry is shown in Fig. 1. The excitation-fluorescence sequence is



The excitation radiation originates from the synchrotron radiation facility at Louisiana State University, the Center for Advanced Microstructures and Devices (CAMD).⁹ The synchrotron radiation is monochromatized by a 6 m plane grating monochromator (PGM).¹⁰ The monochromator was operated in the high-throughput mode for the experiments described here, resulting in an energy bandwidth (ΔE) that was typically 0.5 eV. The degree of linear polarization of the incident radiation is estimated to be approximately 95% near threshold, gradually dropping to 75% at $h\nu_{\text{exc}} = 230$ eV. The results shown below are corrected for the incomplete polarization of the incident radiation. The excitation radiation passes through a two-stage capillary differential pumping system, which guides the vacuum ultraviolet (VUV) radiation to the interaction region and maintains the ultrahigh vacuum integrity of the beam line and electron storage ring. The VUV radiation intersects the gas sample, which emerges from an effusive free-jet expansion. An effusive gas source is used rather than a supersonic jet in order to keep the neutral target molecules rotationally hot (250–290 K). This facilitates the analysis by enabling the high- J limiting expressions to be used.¹¹ The background gas pressure in the chamber was maintained at 6×10^{-4} Torr for the measurements presented here, and we also checked the results at lower pressures to ensure that the data were free of artifacts due to secondary processes.⁸ We estimate that the effective pressure in the interaction region is 10–100 times greater than the background chamber pressure. The fluorescence optics are

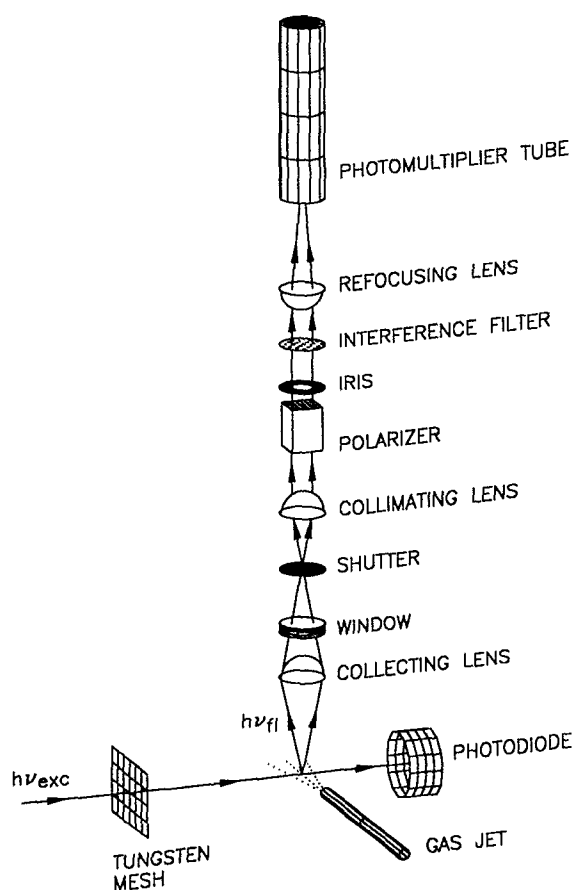
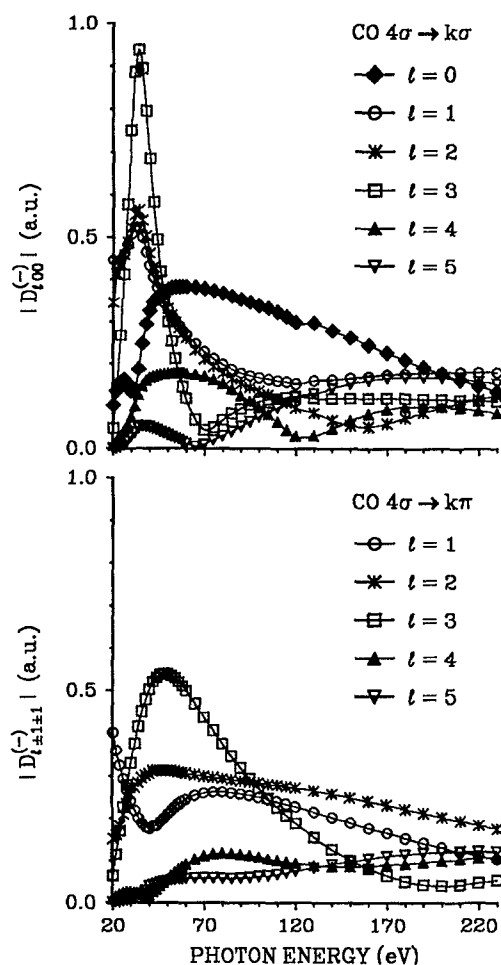


FIG. 1. Experimental schematic.

sketched in Fig. 1. The optical layout is more complex than that used in previous studies because the $\text{CO}^+(B^2\Sigma^+ \rightarrow X^2\Sigma^+)$ fluorescence is in the ultraviolet ($\lambda_{fl} \approx 2200 \text{ \AA}$), necessitating the use of a crystal polarizer (Karl Lambrecht model TFPC-12). The fluorescence radiation was collected by a plano-convex lens and collimated by a second lens before passing through the polarizer. An interference filter was used to reject the $\text{CO}^+(A^2\Pi \rightarrow X^2\Sigma^+)$ fluorescence as well as atomic and atomic ion fluorescence resulting from photodissociation processes. The polarization analyzer, the excitation monochromator, and the vacuum ultraviolet photodiode were controlled via CAMAC and serial links to a PC, similar to data acquisition procedures described previously.^{1,6,7} A more complete description of the experimental details will be given elsewhere.¹²

Calculations were performed in order to help unravel the photoelectron dynamics. Final-state photoelectron wave functions were generated for the $4\sigma \rightarrow k\sigma$ and $4\sigma \rightarrow k\pi$ channels. Figure 2 shows calculated values of the photoelectron matrix elements $|D_{li}^{(-)}|$ for the partial waves in both continuum channels ($i=0$ for $k\sigma$ and $i=\pm 1$ for $k\pi$). The ℓ -composition of these matrix elements clearly shows that the photoionization dynamics exhibited here is far from atomiclike, even at the highest energies. With the strong p character of the 4σ orbital [14.6% s , 62.3% p , 15.7% d , 2.7% f , and 2.7% g ($\ell_0=4$)] at $R_e=2.1322 \text{ a.u.}$, dominant s

FIG. 2. Calculated magnitudes of dipole strengths for individual partial waves for $4\sigma^{-1}$ photoionization of CO.

($\ell=0$) and d ($\ell=2$) photoelectron contributions would be expected on the basis of an atomiclike propensity rule. The calculations were performed at the Hartree–Fock level, and the photoelectron orbitals were obtained by numerical solution of the Lippmann–Schwinger equations using an iterative procedure, based on the Schwinger variational principle.¹³ Details will be given elsewhere.¹²

The results of the experiments and theory are shown in Fig. 3. The bottom frame shows the polarization data, along with predictions from theory. The top frame shows the ratio of dipole strengths, i.e., the relative strengths of the degenerate ionization channels. The dipole strengths are defined as $D_\sigma^2 \equiv \sum_l |D_{l00}^{(-)}|^2$ and $D_\pi^2 \equiv \sum_l |D_{l\pm 1\pm 1}^{(-)}|^2$, and the ratio R defines the relative strengths, i.e., $R \equiv D_\pi^2/D_\sigma^2$. The experimental results are in excellent agreement with results obtained previously over a more limited spectral range.³ We focus our attention on two aspects of these data. First, there is a resonant feature at $h\nu_{exc} \approx 37 \text{ eV}$. This is a $4\sigma \rightarrow k\sigma$ shape resonance which has been observed¹⁴ and identified^{15,16} previously. This is the first time that polarization has been observed as a useful probe of labeling (or confirming) the symmetry of a shape resonance. Secondly, the magnitude of

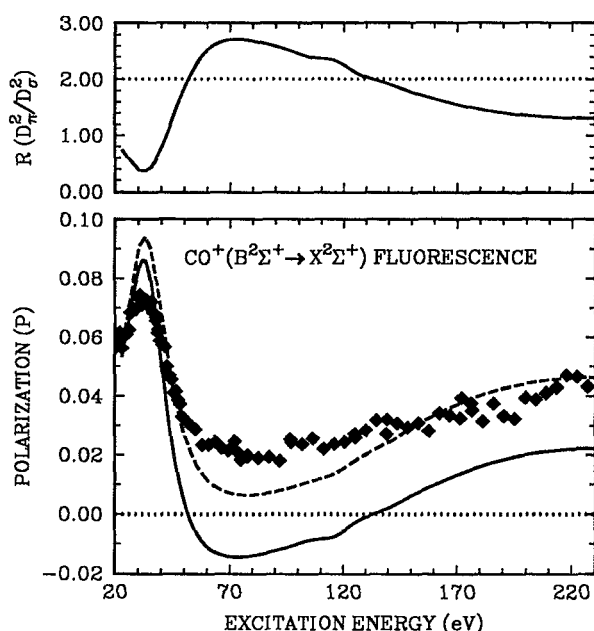


FIG. 3. Bottom frame: measured fluorescence polarization data and predictions from theory. Dashed line: quantum theory results from Eq. (2). Solid line: semiclassical results from Eq. (5). Top frame: calculated ratio of dipole strengths.

the polarization does not approach zero even for energies beyond 230 eV. As a point of reference, note that the ionization potential for the $\text{CO}^+(B^2\Sigma^+)$ state is 19.7 eV,¹⁷ so the highest photoelectron energies are more than 210 eV (i.e., more than ten times the binding energy) and the photoions are still produced with considerable alignment.

In order to extract useful insights from these data, it is helpful to review the physical basis of fluorescence polarization from molecular photoions.^{1,3–8,11} As Eq. (1) indicates, an electron ejected from the CO 4σ orbital can exit via the $k\sigma$ or $k\pi$ continuum channels. Ejection through the $k\sigma$ channel results in an electron-ion complex that has Σ^+ final-state symmetry, while ejection into the $k\pi$ continuum produces an electron-ion complex with Π symmetry. The key point is that the absorption transition dipole tilts relative to the plane of rotation depending on the relative strengths and interference between partial waves of the competing channels, thereby modulating the degree of alignment.¹¹ Classically, the alignment is a measure of the spatial anisotropy of angular momentum vectors, or quantum mechanically, it is a measure of the unequal populations of available M_J sublevels. The alignment, $\langle A_0^{(2)}(J) \rangle$, ranging from 2 to -1 ,^{11,18,19} is determined by

$$\langle A_0^{(2)}(J) \rangle = \frac{\sum_{M_J} [3M_J^2 - J(J+1)] \sigma(J, M_J)}{J(J+1) \sum_{M_J} \sigma(J, M_J)}, \quad (2)$$

where $\sigma(J, M_J)$ is the total cross section for the M_J sublevel of the J level. Details of calculations for $\sigma(J, M_J)$ are given elsewhere.¹² If we work in the high- J limit, there is a simple relationship between the alignment and the fluorescence polarization of the $\Sigma \rightarrow \Sigma$ fluorescence.¹¹

$$\langle A_0^{(2)} \rangle = \frac{-8P}{3-P}, \quad (3)$$

where $\langle A_0^{(2)} \rangle$ denotes a high- J thermal average.

In our calculations of the alignment parameter $A_0^{(2)}(J^+)$ of Eq. (2) for the J^+ level of the $B^2\Sigma^+$ state of CO^+ , we assume a rotational temperature of 250 K for the CO neutral ground state. To calculate the polarization P of Eq. (3), $\langle A_0^{(2)} \rangle$ is determined by averaging over all $A_0^{(2)}(J^+)$ with $N^+ \geq 10$. Here N^+ is the total angular momentum exclusive of spin for the $B^2\Sigma^+$ state of CO^+ and $J^+ = N^+ \pm 1/2$. Such an average is appropriate since Eq. (3) is only valid in the high- J limit and the $A_0^{(2)}(J^+)$ are approximately the same for both $J^+ = N^+ + 1/2$ and $J^+ = N^+ - 1/2$ levels for high N . $\langle A_0^{(2)} \rangle$ is not sensitive to the actual values of N^+ included in this averaging provided N^+ is not too close to zero. The resulting calculated polarizations (dashed line of Fig. 3) are in excellent agreement with the measured values.

The results in Fig. 3 support the primary conclusion of this study. Specifically, both the experimental data and the theoretical predictions in Fig. 3 show clearly that the dipole strength ratio does not approach the statistical value ($R=2$), nor does the alignment tend toward zero. Thus, the CO photoelectron dynamics exhibit molecular fingerprints even at the highest measurable photoejection energies. It must be emphasized that the degree of alignment is considerable, even though the magnitude of the fluorescence polarization is small. While the alignment parameter for a general system is constrained to the range $-1 \leq \langle A_0^{(2)} \rangle \leq 2$, a freely rotating target system is constrained (in the semiclassical limit) to take on values $-2/5 \leq \langle A_0^{(2)} \rangle \leq +1/5$. The observed polarization at the highest energies is $P \sim 0.04$, which corresponds to $\langle A_0^{(2)} \rangle \approx -0.11$, i.e., the alignment parameter is more than 25% of its limiting value. Moreover, the polarization shows no sign of approaching zero as the photon energy increases, either in the calculations or the experiment.

It is also instructive to examine the limiting values for $\langle A_0^{(2)} \rangle$ and P , assuming that the plane of rotation does not change during the absorption or emission process.^{1,3} This type of approximation has been useful in previous studies^{1,3,7,8} over limited spectral ranges, and it is useful to test the range of validity of such treatments. For a pure $4\sigma \rightarrow k\sigma$ excitation, the absorption transition is $\Sigma \rightarrow \Sigma$, and the transition dipole lies parallel to the internuclear axis.²⁰ One can show that this $4\sigma \rightarrow k\sigma$ pathway results in $\langle A_0^{(2)} \rangle = -2/5$ and $P = +1/7$. On the other hand, a pure $4\sigma \rightarrow k\pi$ excitation is a $\Sigma \rightarrow \Pi$ transition, and the absorption dipole lies perpendicular to the internuclear axis. In this case, $\langle A_0^{(2)} \rangle = +1/5$ and $P = -1/13$. For a realistic situation (neither pure $k\sigma$ or pure $k\pi$), there is a simple semiclassical relation between the dipole strength ratio R and $\langle A_0^{(2)} \rangle$.³

$$R = \frac{2 + 5\langle A_0^{(2)} \rangle}{1 - 5\langle A_0^{(2)} \rangle}. \quad (4)$$

Equation (4) is commonly used to relate the fluorescence polarization to the relative strengths of the degenerate pathways.^{1,3} Specifically, Eqs. (3) and (4) can be combined to obtain the relationship between R and P .

$$R = \frac{2 - 14P}{1 + 13P} \quad (5)$$

This result allows us to convert fluorescence polarizations to ratios of dipole strengths and vice-versa. It should be noted that this formula assumes that the photoelectron dynamics do not influence the molecular rotation significantly, i.e., the semiclassical approximation. It is clear that this simplification is not true at the higher photon energies employed in this study, as the change in angular momentum ($\Delta N = N^+ - N_0$) is not small compared to the target angular momentum at the higher photon energies.²¹ Figure 3 shows the semiclassical values (solid line) of the polarization obtained from Eq. (5) using values of R derived from the calculated dipole matrix elements (D_σ^2 and D_π^2). It is clear that the ratio of dipole strengths is sufficient to predict the trends in the polarization spectra, lending additional credence to the qualitative conclusions obtained from the rigorous results obtained from Eq. (2). However, these semiclassical results differ considerably from the measured values since these simple treatments do not adequately account for effects of angular momentum transfer upon photoionization or interference among partial waves. While the qualitative trends in the polarization values are the same, this comparison indicates that the commonly used semiclassical approach is accurate only at lower energies.

While the utility of fluorescence polarization determinations has been described previously, the present study is the first to provide the basis for qualitative and quantitative tests at extremely high electron kinetic energies. As a result, these data have implications for work beyond the immediate study. For example, the EXAFS phenomenon owes its existence to the detailed behavior of the photoelectron wave function at high kinetic energies. The procedures used to analyze EXAFS data are predicated on a very simple form for the photoelectron wave function that emphasizes the spherical (i.e., atomiclike) aspects of the photoelectron wave function.²² The present results can be extended to test the validity (or more precisely, the range of validity) of such simplifying assumptions.

In conclusion, these data reiterate a useful lesson, namely, that spanning a wide range of scattering energies is essential for probing the dynamics. Experimental probes capable of spanning a wide range are not common.²¹ Fluorescence polarization studies are well suited for viewing the photoejection dynamics in a global context, as the experimental sensitivity is very high, and it is possible to extract physically meaningful insight from the data that naturally cast themselves into the molecular framework. We have also performed analogous experiments and calculations on N_2 , which will be reported elsewhere¹² along with a more detailed discussion of the CO results. The N_2 results corroborate the principal conclusions drawn from the CO data. All of

these studies emphasize that fluorescence polarization studies can be extremely useful for mapping out qualitatively revealing aspects of the photoionization dynamics, particularly aspects which are uniquely molecular in character, and which extend deep into the ionization continua.

The efforts of the CAMD staff are greatly appreciated, and we are particularly indebted to Dr. Volker Saile, Dr. John Scott, and Dr. Eizi Morikawa for their support with the plane grating monochromator. E.D.P. also acknowledges support from NSF (Grant No. CHE-9315857) and the Louisiana LEQSF program. Work at the California Institute of Technology was supported by grants from the Air Force Office of Scientific Research and the Office of Health and Environmental Research of the U.S. Department of Energy. We also acknowledge use of resources of the Jet Propulsion Laboratory/Caltech CRAY Y-MP2E/232 Supercomputer.

^aDepartment of Physics and Astronomy.

^bCenter for Advanced Microstructures and Devices.

^cDepartment of Chemistry.

^dContribution No. 8946.

¹E. D. Poliakoff, J. L. Dehmer, D. Dill, A. C. Parr, K. H. Jackson, and R. N. Zare, *Phys. Rev. Lett.* **46**, 907 (1981).

²J. Cooper and R. N. Zare, *J. Chem. Phys.* **48**, 942 (1968); J. Cooper and R. N. Zare, in *Lectures in Theoretical Physics*, edited by S. Geltman, K. T. Mahanthappa, and W. E. Brittin (Gordon and Breach, New York, 1969), Vol. XI-C, pp. 317-337.

³J. A. Guest, K. H. Jackson, and R. N. Zare, *Phys. Rev. A* **28**, 2217 (1983).

⁴J. A. Guest, M. A. O'Halloran, and R. N. Zare, *J. Chem. Phys.* **81**, 2689 (1984).

⁵J. A. Guest, M. A. O'Halloran, and R. N. Zare, *SSRL Activity Report* (1983).

⁶E. D. Poliakoff, J. L. Dehmer, A. C. Parr, and G. E. Leroi, *J. Chem. Phys.* **77**, 5243 (1982).

⁷E. D. Poliakoff, J. L. Dehmer, A. C. Parr, and G. E. Leroi, *J. Chem. Phys.* **86**, 2557 (1987).

⁸J. W. Keller, W. T. Hill, D. L. Ederer, T. J. Gil, and P. W. Langhoff, *J. Chem. Phys.* **87**, 3299 (1987).

⁹B. C. Craft, M. Feldman, E. Morikawa, E. D. Poliakoff, V. Saile, J. D. Scott, and R. L. Stockbauer, *Rev. Sci. Instrum.* **63**, 1561 (1992).

¹⁰E. Morikawa, J. D. Scott, E. D. Poliakoff, R. L. Stockbauer, and V. Saile, *Rev. Sci. Instrum.* **63**, 1300 (1992).

¹¹C. H. Greene and R. N. Zare, *Annu. Rev. Phys. Chem.* **33**, 119 (1982).

¹²R. Das, C. Wu, A. G. Mihill, E. D. Poliakoff, K. Wang, and V. McKoy (in preparation).

¹³R. R. Lucchese, G. Raseev, and V. McKoy, *Phys. Rev. A* **25**, 2572 (1982).

¹⁴E. W. Plummer, T. Gustafsson, W. Gudat, and D. E. Eastman, *Phys. Rev. A* **15**, 493 (1977).

¹⁵S. Kakar, H. C. Choi, and E. D. Poliakoff, *Chem. Phys. Lett.* **190**, 489 (1992).

¹⁶S. Kakar, H. C. Choi, and E. D. Poliakoff (in preparation).

¹⁷K. P. Huber and G. Herzberg, in *Constants of Diatomic Molecules* (Van Nostrand-Reinhold, New York, 1979).

¹⁸U. Fano and J. H. Macek, *Rev. Mod. Phys.* **45**, 553 (1973).

¹⁹R. N. Zare, *Angular Momentum* (Wiley, New York, 1988).

²⁰G. Herzberg, *Spectra of Diatomic Molecules* (Van Nostrand-Reinhold, New York, 1950).

²¹H. C. Choi, R. Rao, A. G. Mihill, S. Kakar, E. D. Poliakoff, K. Wang, and V. McKoy, *Phys. Rev. Lett.* **72**, 44 (1994).

²²*X-Ray Absorption: Principles, Applications, and Techniques*, edited by D. C. Koningsberger and R. Prins (Wiley, New York, 1988).